

## 0.1 Introduction

Ion channels are transmembrane proteins that transport ions outside of the cell to the inside of the cell. Pentameric ligand gated ion channels (pLGICs) are ion channels made of 5 subunits and gated by various ligands such as neurotransmitters, drugs, and modulated by lipids. pLGICs are divided into three major segments: the extra-cellular domain (ECD), the transmembrane domain (TMD), and the poorly understood inter-cellular domain (ICD), see Figure 1. The ECD is composed of beta-sheets, with ligand binding pockets usually at inter-subunit regions. The TMD spans the membrane. Each subunit is made of 4 alpha-helices, M1 to M4. Alpha-helices M1 and M3 form the 'body' of the TMD, M2 makes up the channel's pore, and M4 protrude into the membrane, and are in constant direct contact with lipids.

pLGICs are essential proteins dedicated to neuronal function. In mammals pLGICs are found in both the central and peripheral nervous system. pLGICs play various roles in neurological diseases related to inflammation Taly et al. (2009); Cornelison et al. (2016); Patel et al. (2017b); Yocum et al. (2017); Egea et al. (2015), addiction Cornelison et al. (2016), chronic pain Xiong et al. (2012), Alzheimer's Disease Walstab et al. (2010); Picciotto & Zoli (2008); CM et al. (1999); Kalamida et al. (2007b), spinal muscular atrophy Arnold et al. (2004), schizophrenia Haydar & Dunlop (2010); Kalamida et al. (2007b) and neurological autoimmune diseases Lennon et al. (2003); Kumari et al. (2008).

There are 4? species of eukaryotic pLGICs: cationic and anionic. Cationic pLGICs, such as nicotinic acetylcholine receptors (nAChRs) and serotonin receptors (5-HT<sub>3</sub>R) are responsible for stimulating action potential along axons. Anionic pLGICs, such as  $\gamma$ -aminobutyric acid type A (GABA<sub>A</sub>R) and glycine receptors (GlyR), are responsible for inhibiting action potentials.

pLGICs are sensitive to their local lipid composition, especially nAChR.

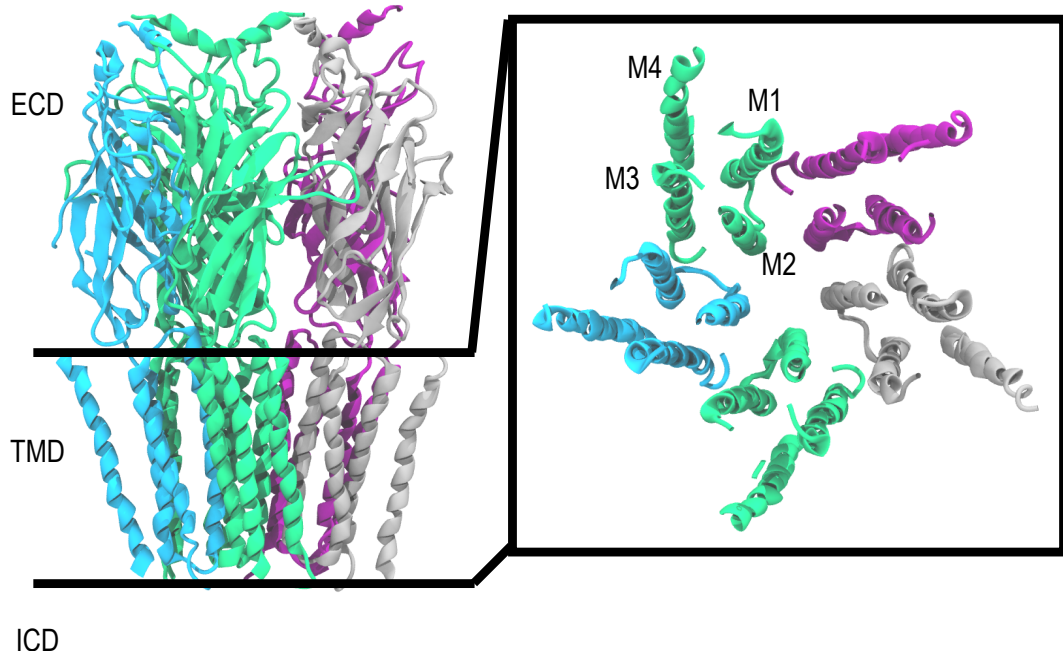


Figure 1: The pLGIC structure nAChR. Structure shown from a side view on the left. ECD is comprised of beta sheets. TMD are alpha helices. The ICD is disordered and not show. The TMD looking down from the ECD. M1 and M3 make up a cylindrical "body" of the channel. M2 makes up the central pore. M4 directly interact with lipids, and provide the conical/star shape.  $\alpha$ : green,  $\gamma$ : blue,  $\delta$ : grey,  $\beta$ : purple.

Experimental approaches to analyze pLGIC membrane domain and boundary lipid composition have relied heavily on model membranes. Model membranes are man made membranes usually consisting of 1 to 3 lipids. Cholesterol and anionic lipids are frequently used and are important for modulating nAChRfunction. Cholesterol in particular plays a number of roles in membranes beyond binding to pLGICs. Cholesterol decreases membrane permeability and the average area per lipid, and adds order to the bulk membrane Yeagle (2016b). The ordering effect of cholesterol on membranes can result in membrane domain formation, if other domain forming lipids are present. Domain formation is the de-mixing of ordered

saturated lipids and cholesterol from less ordered unsaturated lipids, forming liquid ordered ( $l_o$ ) and liquid disordered ( $l_{do}$ ) domains respectively. These domains can form a lipid reservoir of favorable boundary lipids.

Model membranes are useful tools for developing predictive boundary lipid models, but they lack the lipid diversity of a plasma membrane. Model organisms, such as *Xenopus* oocyte may have more than thirty phospholipid speciesGamba et al. (2005); Ferreira et al. (2010). pLGIC native membranes, such as neuronal membranes or *Torpedo* electric organs have more than 30 species of phospholipid ?Taguchi & Ishikawa (2010); ?); Ingólfsson et al. (2017); ?); Quesada et al. (2016). Lipid diversity is not enough though, nAChR when placed in *Xenopus* oocyte have poor function and require lipid additives to conduct ions. This suggests there are specific lipids required for nAChR function not found in *Xenopus* oocyte or not enough of these specific lipids to play a boundary role. A hypothesized essential boundary lipid acyl-species are n-3 polyunsaturated fatty acids (PUFAs).n-3 PUFAs compose  $\sim 15 - 20\%$  of phospholipids found in pLGICnative membranes, but only  $\leq 10\%$  in *Xenopus* oocytes.

### Missing parts still Bullet 3

pLGICs are modulated by their boundary lipid composition. Cholesterol, saturated, and monounsaturated lipids, with neutral or anionic head groups, have been studied the most. how do lipids modulate function??? Cholesterol has been a key lipid of study. In model membranes a minimum of 10 – 20% cholesterol was required to return function to nAChR.

### Bullet 4, kind of 5 too...

The structure and sequence of pLGICs dictates where specific lipids will bind. The M4 alpha-helices have the highest probability to interact with unsaturated lipids and cholesterol. It is hypothesized that PUFAs minimize the membrane deformation caused by the M4 alpha-helices' conical-star shape need pic, and cholesterol helps stabilize the structure. Inter-subunit sites have the

highest probability to interact with saturated lipids, n-3 PUFAs, and cholesterol. We hypothesize n-3 PUFAs and cholesterol stabilize the protein's structure, and saturated lipid's low flexibility fit interact favorably with pLGIC's cylindrical inter-subunit sites. The sequence of the pLGIC's structure dictates the location of anionic lipid binding. The prokaryotic pLGICELIC's inner inter-subunit sites tend to be occupied by anionic lipids, however nAChR's inner M4 sites tend to be occupied by anionic lipids.

pLGICs reconstituted or [grown/injected](#) into model membranes, or model organisms, have boundary lipid compositions not optimized for function. The model organism, *Xenopus* oocyte, has more n-6 and fewer n-3 PUFAs than neuronal membranes. A result of this is n-6 PUFAs tend occupy the M4 region in greater numbers than n-3 PUFAs. *Xenopus* oocyte also have ~ 21% cholesterol versus ~ 40% cholesterol in neuronal membranes. The difference in cholesterol results in a drop in boundary cholesterol density. These composition changes may be the cause of the decrease in function, and increased membrane deformation.

It is experimentally challenging to capture the boundary lipid composition of pLGICs, as well as other membrane channels. Functional experiments, such as electrophysiology and florence quenching, demonstrated anionic lipids and cholesterol as lipid modulated pLGIC's function Ellena et al. (1983); Fong & McNamee (1986b); ?); Jones & Mcnamee (1988); Sunshine & McNamee (1994); DaCosta et al. (2009), but pLGICs are functional dependent on boundary cholesterol Dalziel et al. (1980); Addona et al. (1998); Criado et al. (1983). Structural biology such as cryo-EM, x-ray crystallography, and mass spectrometry, has found potential cholesterol sites at the subunit interface Laverty et al. (2017); Budelier et al. (2019), potential specific phospholipid sites in the inter-subunit site Hénault et al. (2019); Basak et al. (2017) and inter-subunit sites sites Kim et al. (2020), and anionic lipids binding to inner inter-subunit sites Tong et al. (2019). MD simulations are used as a computational tool to visualize below the diffraction

limit and visualize and predict, protein-lipid interactions. MD simulation has identified cholesterol Brannigan et al. (2008a); Woods et al. (2019) interaction at inter-subunit sites and PUFA sites at M4 sites Woods et al. (2019), as well as anionic lipids binding at inner inter-subunit sites Tong et al. (2019).

Predicting boundary pLGIC boundary lipid and specific sites of protein occupancy has been exhaustedly done in model membranes or model organism. These model membranes have provided invaluable predictive models, however pLGIC native boundary lipids are unknown. This thesis is the accumulation for four projects predict pLGIC boundary lipids in coarse-grained model and quasi-realistic membranes. Chapter 1 looks at where nAChR resides in domain forming membranes. Chapter 2 compares domain and non-domain forming membranes for multiple nAChR and predicts locations for lipid occupancy. Chapter 3 is computational work from a collaborative project, predicting anionic occupancy sites for the pLGIC ELIC. Chapter 4 embeds nAChR in a quasi-native membrane, and using the predicted occupancy sites from chapters 2 and 3, calculates the binding affinity of acyl-chain saturation and head group charge.

## Chapter 3

### ***Computational approaches in Direct binding of phosphatidylglycerol at specific sites modulates desensitization of a ligand-gated ion channel***

#### **3.0.1 Introduction**

pLGICs are a family of essential proteins evolved for neuronal function. pLGICs are gated by various neurotransmitters, but are functionally modulated by their boundary lipid composition. The well studied pLGIC nAChR conducts cations across the membrane to stimulate an action potential, and is functionally dependent on cholesterol and anionic lipids Dalziel et al. (1980); Ellena et al. (1983); Criado et al. (1983); Fong & McNamee (1986b); ?); Jones & McNamee (1988); Sunshine & McNamee (1994); DaCosta et al. (2009). Lipid binding sites for pLGICs are still relatively unknown.

Structural biology has predicted cholesterol and fatty acid binding sites in pLGICs Laverty et al. (2017); Basak et al. (2017). Coarse grained molecular dynamics (CGMD) work by SharpSharp et al. (2019) and WoodsWoods et al. (2019) predicted cholesterol binding sites around nAChR. pLGIC-anionic lipid binding sites are still unknown. This work is the computational portion of a collaborative project predicting anionic binding site for the pLGIC *Erwinia* ligand-gated ion channel (ELIC). Using CGMD as a computational microscope and simulating ELIC in membranes comprised of neutral and anionic lipids we visualize and test potential anionic-ELIC binding distributions from native mass spectrometry studies performed by Tong et al. (2019).

### 3.0.2 Computational Methods

All simulations reported here used the MARTINI 2.2 Marrink et al. (2007a) coarse-grained topology and force field. The crystal structure of ELIC (PDB 3RQW) (62) was coarse-grained using MARTINI martinize.py script. Secondary structural restraints were constructed using martinize.py while imposed through Gromacs (63). Conformational restraints were preserved through harmonic bonds between backbone beads less than 0.5 nm apart with a coefficient of 900 kJ mol<sup>-1</sup>. Pairs were determined using the ElNeDyn algorithm (64). Membranes were constructed using the MARTINI script insane.py (61). The insane.py script randomly places lipids throughout both inner and outer membranes and embeds selected proteins into the membrane. Two series of simulations were developed, the first using POPE and POPG, and the second POPC and POPG. Box sizes were about 30 x 30 x 25 nm<sup>3</sup> and each simulation box contained about 3000 lipids.

Molecular dynamics simulations were carried out using GROMACS 5.1.4 Berendsen et al. (1995). All systems were run using van der Waals (vdW) and electrostatics in cutoff and reaction-field, respectively, with a dielectric constant of  $\epsilon = 15$ . vdW and electrostatics used a cutoff length of 1.1 nm as defined in current MARTINI build specifications. Energy minimizations were performed for about 30,000 steps. All systems were run for short equilibration steps. Canonical ensembles (NVT) were run for 100 ps using Berendsen thermostat set to 323 K with the temperature coupling constant set to 1 ps. Isothermal-Isobaric ensemble (NPT) equilibration was run for 5000 ps using Berendsen thermostat and barostat. The thermostat was set to 323 K with the temperature coupling constant set to 1 ps, and the barostat was set to a pressure coupling constant of 3 ps with a compressibility of  $3 \times 10^{-5}$  bar<sup>-1</sup> holding at 1 bar. Molecular dynamics were carried out using NPT ensemble and were simulated for 15  $\mu$ s with a time step of 0.015 ps using v-rescale thermostat set to 323 K and a temperature coupling constant of 1 ps. Membranes consisting of POPE used the Parrinello-Rahman barostat, and

membranes consisting of POPC used the Berendsen barostat, both under semi-isotropic coupling. The reference pressure was set to 1 bar, the compressibility  $3 \times 10^{-4} \text{ bar}^{-1}$ , and the pressure coupling constant 1 ps.

Annular lipids were determined using the annular lipid metric B:

$$B_i = \left\langle \frac{b_i}{b_{\text{tot}}} \right\rangle \frac{1}{x_i} - 1 \quad (3)$$

where  $b_i$  is the instantaneous number of boundary lipids of species  $i$ ,  $b_{\text{tot}}$  is the instantaneous total number of boundary lipids,  $x_i$  is the overall (bulk) fraction of species  $i$  and the brackets represent an average over time and replicas.  $B_i < 0$  and  $B_i > 0$  indicate enrichment and depletion of species  $i$ , respectively, relative to the abundance in the bulk membrane. A given lipid was counted as a boundary lipid if it was within 6 Å of the ELIC transmembrane domain.

Two dimensional lipid density distributions around a central ELIC pentamer were calculated for each leaflet using polar coordinates (28). For every sampled frame, all lipids of species  $i$  were separated into leaflets. For all  $i$  lipids in a given leaflet, the vector separating the phosphate beads from ELIC center was calculated and projected onto the membrane plane. The two-dimensional separation vector was then used to assign the lipid to the appropriate polar bin of radial bin width 4 Å and angular bin width  $\frac{\pi}{15}$ . The area density in each bin was averaged over time and replicas.

### 3.0.3 Computational Results

To further examine phospholipid interactions with ELIC using a molecular model, coarse-grained MD simulations were performed on binary POPG/POPC and POPG/POPE model membranes containing a single ELIC pentamer (Fig. 2A). Unlike fully-atomistic simulations, coarse-grained simulations permit significant diffusion of lipids over simulation time scales. The boundary lipid composition can thus equilibrate over the simulation time, even if it varies significantly from the bulk membrane composition. The POPG fraction was varied between 0 and 70%.

Enrichment or depletion of POPG among boundary lipids for each concentration was quantified using the boundary lipid metric B (Equation 3, see Methods). For a given lipid species,  $B > 0$  reflects enrichment,  $B < 0$  reflects depletion, and  $B = 0$  reflects random mixing. For POPG,  $B > 0$  for all compositions tested (Fig. 2B). This result indicates that if POPG is present in the membrane, it is enriched among boundary lipids. This enrichment is strongest for lower amounts of POPG (i.e. lower  $x_{\text{POPG}}$ ), consistent with specific binding of POPG to ELIC.

We further examined these sites of interaction using our coarse-grained MD simulations. To identify whether boundary POPG were localized around specific helices or residues, two-dimensional densities of the negatively-charged headgroup bead were calculated. The distributions are separated by leaflet where each leaflet contained 10% POPG. As shown in Figure 5A, POPG was more likely to interact with ELIC in the inner leaflet than the outer leaflet, consistent with three out of five interfacial arginines residues being located on the intracellular interface of the ELIC TMD. These three arginines are located on TM3 (R286) and TM4 (R299 and R301). Contacts between POPG and all three of these residues are also visible in individual frames of the simulation (Fig. 5B). Moreover, POPG is more likely to be contacting the interfacial residues in TM4 (such as R299 and R301) than accessible interfacial residues in any other helices (Fig. 5A). The remaining two arginine residues are located at the TMD-ECD interface (R117 and R123). POPG density in the outer leaflet localized to these residues at intrasubunit sites between TM4 and TM1 or TM4 and TM3 (Fig. 5A), and contacts between these residues and POPG headgroups in the outer leaflet were also observed in snapshots from the MD simulations (Fig. 5B). In summary, the native MS data and coarse-grained MD simulations demonstrate that five interfacial arginines contribute to specific POPG binding sites in the inner and outer leaflets adjacent to TM4.

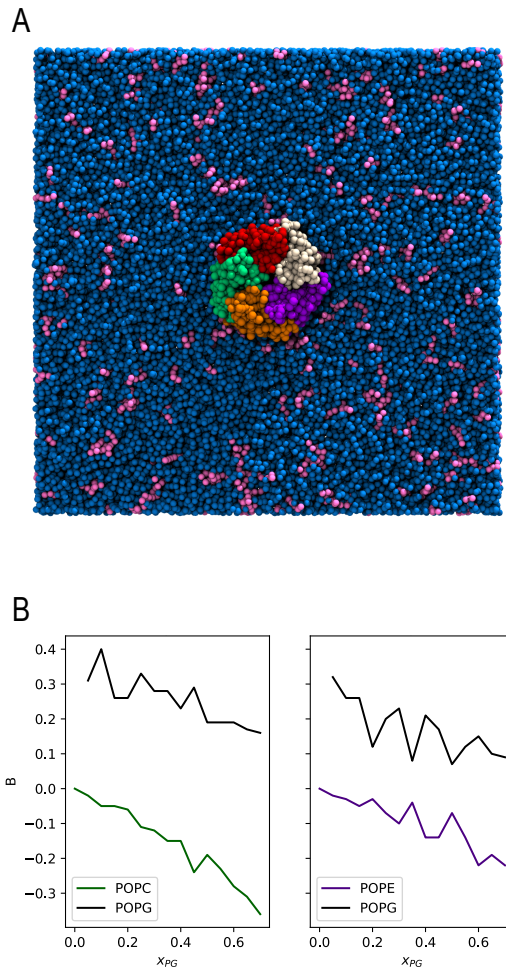


Figure 3.1: Enrichment of POPG among ELIC boundary phospholipids from coarse-grained simulations. (A) Image of the simulation model of ELIC embedded in a membrane consisting of 10% POPG (pink) and % POPC (blue). The view is from the extracellular side of ELIC perpendicular to the membrane. (B) The boundary enrichment metric,  $B$ , is shown for phospholipid species in POPC/POPG membranes (left) or POPE/POPG membranes (right) over a range of POPG mole fractions ( $x_{PG}$ ).  $B$  is defined in Equation 3 (see Methods) and reflects the fractional difference between the amount of a lipid species found in the boundary and the bulk membrane:  $B > 0$  indicates enrichment,  $B \leq 0$  indicates depletion, and  $B = 0$  indicates no difference in mole fraction between the bulk and the boundary.

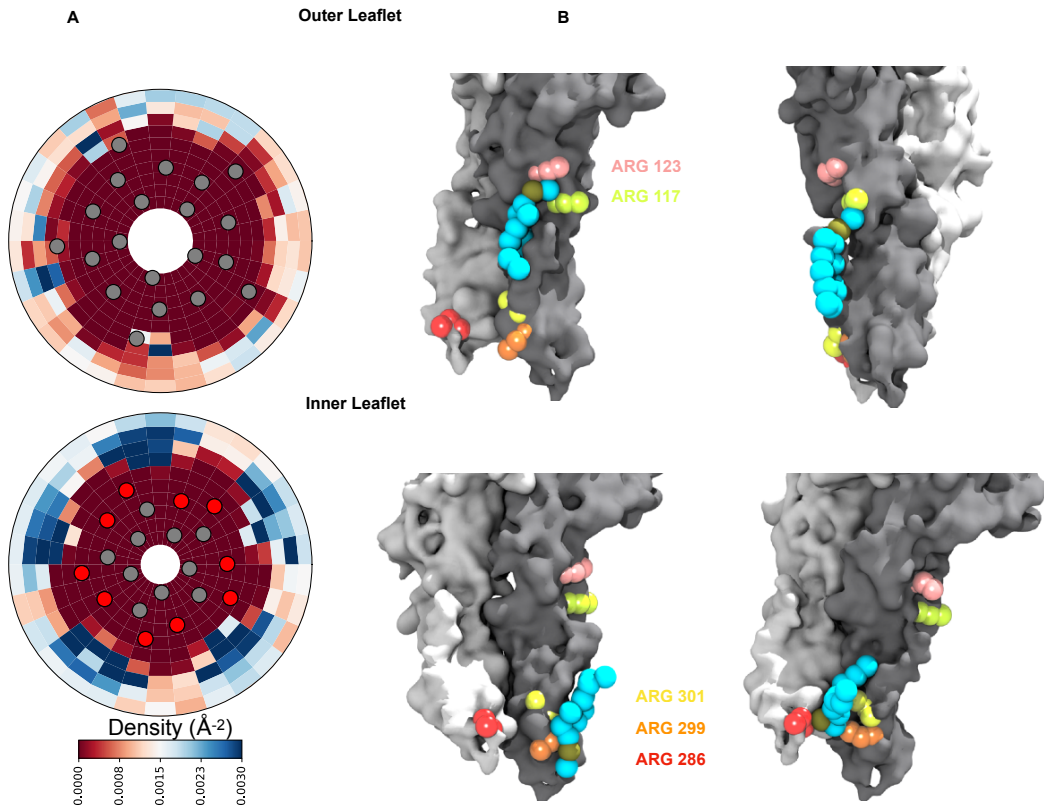


Figure 3.2: Density calculations of lipids in binary membranes and visualization of direct POPG-ELIC interactions at 10% POPG. (A) Distribution of POPG density in a POPG-POPC membrane, within 40  $\text{\AA}$  from the ELIC pore over the last half of a 15  $\mu\text{s}$  simulation, for both the outer leaflet (top) and the inner leaflet (bottom). Density is colored according to the color bar, where red and blue represent low and high POPG density, respectively. Circles represent the ELIC transmembrane backbone center of mass, with the helices containing the interfacial arginines colored in red (B) Representative frames after 9  $\mu\text{s}$  of simulation, showing multiple POPG binding modes associated with high density areas in (A). Two adjacent subunits of ELIC are shown in grey and white, while arginine side chains of interest are colored in peach, lime-yellow, orange, yellow, and red. POPG phosphate is colored in tan with the rest of the lipid in cyan.